This is a “preproof” accepted article for Mineralogical Magazine.
This version may be subject to change during the production process.
10.1180/mgm.2025.19
Revision 1

Svornostite-(NH_4), $(NH_4)_2Mg(UO_2)_2(SO_4)_4(H_2O)_8$, a new mineral from the Blue Lizard mine, San Juan County, Utah, USA, and the establishment of the svornostite mineral group

Anthony R. Kampf[1]*, Travis A. Olds[2], Jakub Plášil[3], Chi Ma[4], Aaron J. Celestian[1] and Joe Marty[1]

[1]Mineral Sciences Department, Natural History Museum of Los Angeles County, 900 Exposition Boulevard, Los Angeles, CA 90007, USA; [2]Section of Minerals and Earth Sciences, Carnegie Museum of Natural History, 4400 Forbes Avenue, Pittsburgh, Pennsylvania 15213, USA; [3]Institute of Physics of the CAS, Na Slovance 1999/2, 18200 Prague 8, Czech Republic and [4]Division of Geological and Planetary Sciences, California Institute of Technology, 1200 East California Boulevard, Pasadena, California 91125, USA

*E-mail: akampf@nhm.org

Abstract

The new mineral svornostite-(NH_4) (IMA2024-068), $(NH_4)_2Mg(UO_2)_2(SO_4)_4(H_2O)_8$, was found in the Blue Lizard mine, San Juan County, Utah, USA, where it occurs as sprays and subparallel groups of yellow blades in a secondary assemblage with ammoniozippeite, blödite, boussingaultite, gypsum, hexahydrite, kröhnkite, plášilite and quartz. The streak is very pale yellow. Crystals are transparent with vitreous lustre. The tenacity is brittle, the Mohs hardness is about 2½, the fracture is curved. The mineral is soluble in H_2O and has a measured density of 3.06(2) $g \cdot cm^{-3}$. The mineral is optically biaxial (+) with $\alpha = 1.560(2)$, $\beta = 1.564(2)$, $\gamma = 1.589(2)$; $2V = 43(1)°$; orientation: X = **a**, Y = **b**, Z = **c**; pleochroism: X colourless, Y yellow, Z yellow; $X < Y \approx Z$. Electron microprobe analyses provided

$[(NH_4)_{1.895}Na_{0.065}K_{0.040}]_{\Sigma 2.000}(Mg_{0.755}Mn_{0.252})_{\Sigma 1.007}(U_{0.996}O_2)_2(S_{1.002}O_4)_4(H_{1.998}O)_8$. Svornostite-($NH_4$) is orthorhombic, $Pmn2_1$, a = 13.0259(9), b = 8.2909(4), c = 11.2589(4) Å, V = 1215.92(11) Å^3 and Z = 2. The crystal structure (R_1 = 0.0243 for 2222 $I > 2\sigma_I$ reflections) contains uranyl-sulfate chains that are linked into sheets by $MgO_2(H_2O)_4$ octahedra and 9- and 10-coordinated NH_4^+ groups. The sheet has the same topology as the sheets in several synthetic uranyl selenates. Svornostite-(NH_4) is a member of the newly established svornostite group, which also includes svornostite-(K), oldsite-(K), rietveldite and zincorietveldite.

Keywords: svornostite-(NH_4); new mineral; svornostite group; uranyl sulfate; crystal structure; svornostite-(K); oldsite-(K); rietveldite; zincorietveldite; Blue Lizard mine, Red Canyon, Utah, USA

Introduction

Svornostite, $K_2Mg(UO_2)_2(SO_4)_4(H_2O)_8$, was described by Plášil *et al*. (2015) from Jáchymov, Czech Republic. They noted that its structure, characterized by $[(UO_2)(SO_4)_2(H_2O)]^{2-}$ uranyl-sulfate chains linked by $MgO_2(H_2O)_4$ octahedra, was very similar to that of a group of synthetic compounds of general formula $M^{2+}(UO_2)(SO_4)_2{\cdot}5H_2O$ (Serezhkin and Serezhkina 1978). Kampf *et al*. (2017) described the mineral rietveldite, $Fe^{2+}(UO_2)(SO_4)_2(H_2O)_5$, from three localities: the Giveaway-Simplot mine (Utah, USA), the Willi Agatz mine (Saxony, Germany) and Jáchymov. The structures of rietveldite and svornostite were noted to be almost equivalent except that one of the octahedrally coordinated Fe sites and two H_2O sites present in the rietveldite structure are missing in the svornostite structure, being replaced by K sites. Kampf *et al*. (2017) also noted that the structures of rietveldite and the synthetic $M^{2+}(UO_2)(SO_4)_2{\cdot}5H_2O$ compounds are polytypes, rietveldite having approximately double the

a cell parameter of the synthetic compounds. Plášil *et al*. (2023) described oldsite, $K_2Fe^{2+}(UO_2)_2(SO_4)_4(H_2O)_8$, from the North Mesa mine group (Utah, USA), which they noted as being the Fe^{2+} analogue of svornostite. That same year, Kampf *et al*. (2023) described the Zn analogue of rietveldite, zincorietveldite, $Zn(UO_2)(SO_4)_2(H_2O)_5$, from the Blue Lizard mine (Utah, USA).

In the current paper, we describe the NH_4 analogue of svornostite, $(NH_4)_2Mg(UO_2)_2(SO_4)_4(H_2O)_8$, which is named svornostite-(NH_4) in line with a new group nomenclature scheme for these closely related minerals. This scheme also involves renaming the original svornostite to svornostite-(K) and the renaming of oldsite to oldsite-(K). The group is to be called the svornostite group and includes two subgroups: (1) the svornostite subgroup with general formula $A^{+}_2M^{2+}(UO_2)_2(SO_4)_4(H_2O)_8$ (Z = 2) and (2) the rietveldite subgroup with general formula $M^{2+}(UO_2)(SO_4)_2(H_2O)_5$ (Z = 4), [or $M^{2+}_2(UO_2)_2(SO_4)_4(H_2O)_{10}$ (Z = 2)], where A is the dominant large monovalent cation and M is the dominant octahedrally coordinated divalent cation. The members of the svornostite subgroup are svornostite-(K), svornostite-(NH_4) and oldsite-(K). The members of the rietveldite subgroup are rietveldite and zincorietveldite. The existing members of the group are listed in Table 1 with selected characteristics for comparison. Note that, to minimize changes in already established names, the naming approach for species in the two subgroups differs. For species in the svornostite subgroup, species with different dominant M cations require different root names and the dominant A cation (generally either K or NH_4) is appended as a suffix. For species in the rietveldite subgroup, the dominant M cation (other than Fe) is indicated as a prefix to the rootname rietveldite.

The new mineral svornostite-(NH_4) and the new group nomenclature were approved by the Commission on New Minerals, Nomenclature and Classification of the International Mineralogical Association (IMA2024-068). The description of svornostite-(NH_4) is based on

four cotype specimens, all micromounts, deposited in the collections of the Natural History Museum of Los Angeles County, 900 Exposition Boulevard, Los Angeles, CA 90007, USA, catalogue numbers 76445, 76446, 76447 and 76448.

Occurrence

Svornostite-(NH_4) was first found in 2012 by one of the authors (JM) underground in the Blue Lizard mine (37°33'26"N 110°17'44"W), Red Canyon, White Canyon District, San Juan County, Utah, USA. The mineral was subsequently found at two other mines in the White Canyon district: in 2015 at the Markey mine in Red Canyon and in 2020 at the Scenic mine in Fry Canyon. The description of the mineral is based only on material from the Blue Lizard mine, which is considered the only type locality. The following information on the mine and its geology is taken largely from Chenoweth (1993).

The deposit exploited by the Blue Lizard mine was first recognized in the summer of 1898 by John Wetherill, while leading an archeological expedition into Red Canyon. He noted yellow stains around a petrified tree. At that spot, he built a rock monument, in which he placed a piece of paper to claim the minerals. Although he never officially recorded his claim, 45 years later, in 1943, he described the spot to Preston V. Redd of Blanding, Utah, who went to the site, found Wetherill's monument and claimed the area as the Blue Lizzard claim (note alternate spelling). Underground workings to mine uranium were not developed until the 1950s.

The uranium deposits in Red Canyon occur within the Shinarump member of the Upper Triassic Chinle Formation, in channels incised into the reddish-brown siltstones of the underlying Lower Triassic Moenkopi Formation. The Shinarump member consists of medium- to coarse-grained sandstone, conglomeratic sandstone beds and thick siltstone lenses. Ore minerals were deposited as replacements of wood and other organic material and

as disseminations in the enclosing sandstone. Since the mine closed in 1978, oxidation of primary ores in the humid underground environment has produced a variety of secondary minerals, mainly sulfates, as efflorescent crusts on the surfaces of mine walls.

Svornostite-(NH_4) is a relatively rare mineral found in association with ammoniozippeite, blödite, boussingaultite, gypsum, hexahydrite, kröhnkite, plášilite and quartz. Uranyl sulfate minerals typically form by hydration–oxidation weathering of primary uranium minerals, mainly uraninite, by acidic solutions derived from the decomposition of associated sulfides (Finch and Murakami, 1999; Krivovichev and Plášil, 2013; Plášil, 2014). Svornostite-(NH_4) and other secondary minerals occurring in the efflorescent crusts of the mines of Red Canyon have formed by such a process. The $(NH_4)^+$ is presumably derived from decaying organic matter and/or from bacterial activity related to the breakdown of the sulfides in the deposit.

Morphology, physical properties and optical properties

Svornostite-(NH_4) occurs in sprays and subparallel groups of yellow blades, up to about 0.5 mm long (Fig.1). Blades are elongate on [001], flattened on {010} and exhibit the forms {100}, {010}, {001}, {00-1}, {110}, {011}, {01-1}, {101}, {-10-1}, {111} and {11-1} (Fig. 2). Merohedral twinning is likely because of the noncentrosymmetric space group. The mineral does not fluoresce under 405 nm ultraviolet illumination. Crystals are transparent with vitreous lustre. The tenacity is brittle and the fracture is curved. The Mohs hardness is about 2½ based on scratch tests. Cleavage is excellent on {010}, good on {100} and fair on {001}. The density measured by flotation in a mixture of methylene iodide and toluene is 3.06(2) $g \cdot cm^{-3}$. The calculated density based upon the empirical formula is 3.097 $g \cdot cm^{-3}$. The mineral is easily soluble in room-temperature H_2O.

Svornostite-(NH_4) is optically biaxial (+) with $\alpha = 1.560(2)$, $\beta = 1.564(2)$ and $\gamma = 1.589(2)$ (measured in white light). The measured $2V$ is 43(1)° from extinction data analysed using EXCALIBRW (Gunter *et al*., 2004). The calculated $2V$ is 44.2°. Dispersion could not be observed. The optical orientation is X = **a**, Y = **b**, Z = **c**. The mineral is pleochroic with X colourless, Y and Z yellow; $X < Y \approx Z$. The Gladstone-Dale compatibility (Mandarino, 2007) $1 - (K_p/K_c)$ is -0.008 (superior) based on the empirical formula using $k(UO_3) = 0.118$, as provided by Mandarino (1976).

Raman Spectroscopy

Raman spectroscopy was done on a Horiba XploRa PLUS micro-Raman spectrometer using an incident wavelength of 532 nm, laser slit of 100 μm, 1800 gr/mm diffraction grating and a 100× (0.9 NA) objective. The spectrum, recorded from 4000 to 60 cm^{-1}, is shown in Figure 3. The spectrum of svornostite-(NH_4) is very similar to those of svornostite (Plášil *et al*., 2015), oldsite (Plášil *et al*., 2023), rietveldite (Kampf *et al*., 2017) and zincorietveldite (Kampf *et al*., 2023). The band assignments indicated in Figure 3 are the same as those previously proposed for svornostite-(K) and oldsite-(K), except that the bands in the 3700-3000 cm^{-1} range are attributed to both ν OH and ν NH. The broad features at 3198 and 3154 cm^{-1} are not observed in the spectra of svornostite-(K), oldsite-(K), rietveldite and zincorietveldite and it is likely that these features are related to $(NH_4)^+$, which is only found in the structure of svornostite-(NH_4). Using the empirically derived equation of Libowitzky (1999), the maxima at 3553, 3531 and 3493 cm^{-1} are consistent with hydrogen bond O···O distances in the range 2.88 – 3.00 Å. This matches well with our proposed hydrogen bonding scheme for which 8 of the 14 O···O distances are in the range 2.90 to 3.05 Å (see Table 5). According to the empirical relationship of Bartlett and Cooney (1989), the ν_1 $(UO_2)^{2+}$ band at 855 cm^{-1} corresponds to an

approximate U–O_{Ur} bond length of 1.76 Å, in good agreement with U–O_{Ur} bond lengths from the X-ray data: 1.762(6) and 1.778(6) Å.

Infrared spectroscopy

Attenuated total reflectance (ATR) Fourier transform infrared (FTIR) spectroscopy for svornostite-(NH_4) was done using a liquid N_2-cooled SENSIR Technologies IlluminatIR mounted to an Olympus BX51 microscope. An ATR objective (ZnSe) was pressed into a crystal grouping and a spectrum measured from 4000 to 650 cm^{-1}. Band assignments provided in Figure 4 are based on those of Čejka (1999), Gurzhyi *et al*. (2024) and Pekov *et al.* (2014). Note, in particular, the medium strong band at 1432 cm^{-1} that is assigned to the N–H bending vibration of $(NH_4)^+$ groups.

Laser Induced Breakdown Spectroscopy

Laser-induced breakdown spectroscopy (LIBS) was done under an argon atmosphere on an Applied Photonics LIBS 8 equipped with a Nitron 1064 nm Q-switched Nd:YAG laser operating at 35 mJ and 10 Hz data acquisition. The spectrum was obtained on a tightly intergrown group of svornostite-(NH_4) crystals approximately 300 μm in diameter. The eight-channel spectrometer collected data from 180 nm to 1022 nm. Peak fitting and identification were performed using the Applied Photonics LIBS instrument software. The portion of the spectrum between 740 and 750 nm where the N I bands appear is shown in Figure 5. Although quantitation was not attempted, a spectrum for ammoniomathesiusite, $(NH_4)_5(UO_2)_4(SO_4)_4(VO_5)\cdot 4H_2O$, was recorded for comparison. It was noted that the N I bands in the two spectra are in the same positions and are of similar intensity.

Chemical composition

Chemical analyses (6) were done at Caltech on a JXA-iHP200F electron microprobe in WDS mode. Analytical conditions were 15 kV accelerating voltage, 5 nA beam current and a beam diameter of 10 μm. Because the blades tend to fragment during polishing, analyses were done on unpolished crystal faces. Although all analyses showed a significant amount of NH_4 to be present, $(NH_4)_2O$ values obtained were highly variable and significantly lower than predicted by the structure determination (0.51–0.82 wt%). The presence of significant amounts of N is strongly indicated by energy dispersive spectroscopy (EDS), FTIR and LIBS. The standardless EDS analyses were consistent with N:(Mg+Mn) ≈ 2. The structure indicates that NH_4 and some of the H_2O are relatively weakly bonded, so it is to be expected that much of these constituents are lost during the EPMA analyses. Insufficient material is available for CHN analysis, so $(NH_4)_2O$ and H_2O are calculated based on the structure (U+S = 6 and O = 28 *apfu*). The low analytical total can be attributed to the fact that the analyses were done on unpolished crystal faces, which exhibited some roughness and were not lying perfectly level. The analytical results are given in Table 2. It should be noted that the possible presence of H_3O^+ substituting for NH_4^+ was discounted because no hydronium-bearing phases have been found in any of the post-mining mineral assemblages in the Blue Lizard mine, or in any of the Red Canyon mines, for that matter.

The empirical formula (based on 28 O *apfu*) is $[(NH_4)_{1.895}Na_{0.065}K_{0.040}]_{\Sigma 2.000}(Mg_{0.755}Mn_{0.252})_{\Sigma 1.007}(U_{0.996}O_2)_2(S_{1.002}O_4)_4(H_{1.998}O)_8$. The simplified formula is $[(NH_4),Na,K]_2(Mg,Mn)(UO_2)(SO_4)_2(H_2O)_8$. The ideal formula is $(NH_4)_2Mg(UO_2)_2(SO_4)_4(H_2O)_8$, which requires $(NH_4)_2O$ 4.61, MgO 3.57, UO_3 50.68, SO_3 28.37, H_2O 12.77, total 100 wt.%.

X-ray crystallography

Powder X-ray diffraction (PXRD) data were recorded using a Rigaku R-Axis Rapid II curved imaging plate microdiffractometer with monochromatized Mo*K*α radiation. A Gandolfi-like motion on the φ and ω axes was used to randomize the sample. Observed *d* values and intensities were derived by profile fitting using JADE Pro software (Materials Data, Inc.). The powder data are presented in Supplementary Table S1. This table is deposited with the Principal Editors of *Mineralogical Magazine* and is available from the online version of the journal at https://www.cambridge.org/core/journals/mineralogical-magazine. The unit-cell parameters refined from the powder data using JADE Pro with whole pattern fitting are (space group $Pmn2_1$) a = 13.044(3), b = 8.2948(18), c = 11.259(2) Å and V = 1218.2(4) Å^3.

The single–crystal structure data were collected at room temperature using the same diffractometer and radiation noted above. The Rigaku CrystalClear software package was used for processing the structure data, including the application of an empirical absorption correction using the multi-scan method with ABSCOR (Higashi, 2001). Systematic absences and E statistics indicated the noncentric space group $Pmn2_1$ (#31). The structure was solved using the intrinsic-phasing algorithm of SHELXT (Sheldrick, 2015a). SHELXL-2016 (Sheldrick, 2015b) was used for the refinement of the structure. The structure solution located all non-hydrogen atoms, which were refined with anisotropic displacement parameters. The N1 and N2 sites were refined with full occupancies by N only. The Mg site was refined with joint occupancies by Mg and Mn yielding $Mg_{0.749(16)}Mn_{0.251(16)}$, almost exactly matching the EPMA results: ($Mg_{0.755}Mn_{0.252}$). The H atom locations could not be found in the difference-Fourier maps. The two highest electron density residuals, 2.03 and 1.75 e Å^{-3}, are at distances of 0.90 and 0.98 Å, respectively, from the U site, indicating that the absorption correction was not completely successful. Data collection and refinement details are given in Table 3, atom

coordinates and displacement parameters in Table 4, selected bond distances in Table 5 and a bond-valence analysis in Table 6.

Description of the structure

In the structure of svornostite-(NH_4), the U site is surrounded by seven O atoms forming a squat UO_7 pentagonal bipyramid. This is the most typical coordination for U^{6+}, particularly in uranyl sulfates, where the two short apical bonds of the bipyramid constitute the uranyl group. Four of the five equatorial O atoms of the UO_7 bipyramid participate in SO_4 tetrahedra; the other is an H_2O group. The linkages of pentagonal bipyramids and tetrahedra form an infinite $[(UO_2)(SO_4)_2(H_2O)]^{2-}$ chain along [001] (Fig. 6). The chains are linked in the [100] direction by $MgO_2(H_2O)_4$ octahedra, which share O vertices with SO_4 tetrahedra in the chains. A heteropolyhedral sheet parallel to {010} is thereby formed. Two $(NH_4)^+$ cations form bonds with O atoms in the chains and octahedra thereby linking the structure in three dimensions (Fig. 7). A network of hydrogen bonds further links the structure.

Svornostite-(NH_4), is isostructural with svornostite-(K), $K_2Mg[(UO_2)(SO_4)_2]_2 \cdot 8H_2O$ (Plášil *et al.*, 2015) and oldsite-(K), $K_2Fe^{2+}[(UO_2)(SO_4)_2]_2(H_2O)_8$ (Plášil *et al.*, 2023). The structures of these three minerals are almost the same as those of rietveldite, $Fe_2(UO_2)_2(SO_4)_4(H_2O)_{10}$ (Kampf *et al*., 2017), and zincorietveldite, $Zn_2(UO_2)_2(SO_4)_4(H_2O)_{10}$ (Kampf *et al*., 2023); however, there are two octahedrally coordinated divalent cation sites in the structures of rietveldite and zincorietveldite and only one in the structures of svornostite-(NH_4), svornostite-(K) and oldsite-(K). Additionally, two H_2O groups in the rietveldite and zincorietveldite structures are replaced with K or $(NH_4)^+$ cations in the svornostite-(NH_4), svornostite-(K) and oldsite-(K) structures. The structures of rietveldite and svornostite-(NH_4) are compared in Figure 6, but the differences (and similarities) are more readily appreciated by comparing the $x = 0$ layers of the structures (Fig. 8).

The $[(UO_2)(SO_4)_2(H_2O)]^{2-}$ chains are essentially identical in the svornostite-(NH_4), svornostite-(K), oldsite-(K), rietveldite and zincorietveldite structures. Topologically identical chains are also found in the structures of bobcookite, $Na(H_2O)_2Al(H_2O)_6[(UO_2)_2(SO_4)_4(H_2O)_2]\cdot 8H_2O$ (Kampf *et al*. 2015a), oppenheimerite, $Na_2(H_2O)_2[(UO_2)(SO_4)_2(H_2O)]$ (Kampf *et al*. 2015b), synthetic $K_2[(UO_2)(SO_4)_2(H_2O)](H_2O)$ (Ling *et al.*, 2010) and synthetic $Mn(UO_2)(SO_4)_2(H_2O)_5$ (Tabachenko *et al.*, 1979). The chains in oppenheimerite and bobcookite are geometrical isomers of the chain in the structures of the svornostite-(NH_4), svornostite-(K), oldsite-(K), rietveldite and zincorietveldite (Fig. 6).

Acknowledgements

Structures Editor Peter Leverett and two anonymous reviewers are thanked for their constructive comments on the manuscript. The EPMA was carried out at the Caltech GPS Division Analytical Facility, which is supported, in part, by NSF Grant EAR-2117942. This study was funded, in part, by the John Jago Trelawney Endowment to the Mineral Sciences Department of the Natural History Museum of Los Angeles County.

References

Bartlett, J.R. and Cooney, R.P. (1989) On the determination of uranium-oxygen bond lengths in dioxouranium(VI) compounds by Raman spectroscopy. *Journal of Molecular Structure*, **193**, 295–300.

Čejka, J. (1999) Infrared spectroscopy and thermal analysis of the uranyl minerals. pp. 521-622. In P.C. Burns, and R.C. Ewing, Eds. *Uranium: Mineralogy, geochemistry and the environment*, **38**, Mineralogical Society of America.

Chenoweth, W.L. (1993) The Geology and Production History of the Uranium Deposits in the White Canyon Mining District, San Juan County, Utah. *Utah Geological Survey Miscellaneous Publication*, **93**–**3**.

Ferraris, G. and Ivaldi, G. (1988) Bond valence vs. bond length in O…O hydrogen bonds. *Acta Crystallographica*, **B44**, 341–344.

Finch, R.J. and Murakami, T. (1999) Systematics and paragenesis of uranium minerals. In: Burns PC, Ewing RC (eds) Uranium: Mineralogy, Geochemistry and the Environment. Mineralogical Society of America and Geochemical Society *Reviews in Mineralogy and Geochemistry*, **38**, pp 91–179.

Gagné, O.C. and Hawthorne, F.C (2015) Comprehensive derivation of bond-valence parameters for ion pairs involving oxygen. *Acta Crystallographica*, **B71**, 562–578.

García-Rodríguez, L., Rute-Pérez, Á., Piñero, J.R. and González-Silgo, C. (2000) Bond-valence parameters for ammonium-anion interactions. *Acta Crystallographica*, **B56**, 565–569.

Gunter, M.E., Bandli, B.R., Bloss, F.D., Evans, S.H., Su, S.C., and Weaver, R. (2004) Results from a McCrone spindle stage short course, a new version of EXCALIBR, and how to build a spindle stage. *The Microscope*, **52**, 23–39.

Gurzhiy, V.V., Kasatkin, A.V., Chukanov, N.V. and Plášil, J. (2024) Uramphite, $(NH_4)(UO_2)(PO_4)\cdot 3H_2O$, from the second world occurrence, Beshtau uranium deposit, Northern Caucasus, Russia: crystal-structure refinement, infrared spectroscopy, and relation to uramarsite. *American Mineralogist*, (in press) https://doi.org/10.2138/am-2024-9313.

Higashi, T. (2001) *ABSCOR*. Rigaku Corporation, Tokyo.

Kampf, A.R., Plášil, J., Kasatkin, A.V. and Marty, J. (2015a) Bobcookite, $NaAl(UO_2)_2(SO_4)_4\cdot 18H_2O$, and wetherillite, $Na_2Mg(UO_2)_2(SO_4)_4\cdot 18H_2O$, two new uranyl sulfate minerals

from the Blue Lizard mine, San Juan County, Utah, USA. *Mineralogical Magazine*, **79**, 695–714.

Kampf, A.R., Plášil, J., Kasatkin, A.V., Marty, J. and Čejka, J. (2015b) Fermiite, $Na_4(UO_2)(SO_4)_3 \cdot 3H_2O$, and oppenheimerite, $Na_2(UO_2)(SO_4)_2 \cdot 3H_2O$, two new uranyl sulfate minerals from the Blue Lizard mine, San Juan County, Utah, USA. *Mineralogical Magazine*, **79**, 1123–1142.

Kampf, A.R., Sejkora, J., Witzke, T., Plášil, J., Čejka, J., Nash, B.P. and Marty, J. (2017) Rietveldite, $Fe(UO_2)(SO_4)_2(H_2O)_5$, a new uranyl sulfate mineral from Giveaway-Simplot mine (Utah, USA), Willi Agatz mine (Saxony, Germany) and Jáchymov (Czech Republic). *Journal of Geosciences*, **62**, 107–120.

Kampf, A.R., Olds, T.A., Plášil, J. and Marty, J. (2023) Zincorietveldite, $Zn(UO_2)(SO_4)_2(H_2O)_5$, the zinc analogue of rietveldite from the Blue Lizard mine, San Juan County, Utah, USA. *Mineralogical Magazine*, **87**, 528–533.

Krivovichev, S.V. and Plášil, J. (2013) Mineralogy and Crystallography of Uranium. In: Burns, P.C. and Sigmon, G.E. (eds) Uranium: From Cradle to Grave. *Mineralogical Association of Canada Short Courses*, **43**, 15–119.

Ling, J., Sigmon, G.E., Ward, M., Roback, N. and Burns, P.C. (2010) Syntheses, structures, and IR spectroscopic characterization of new uranyl sulfate/selenate 1D-chain, 2D-sheet and 3D framework. *Zeitschrift für Kristallographie*, **225**, 230–239.

Libowitzky, E. (1999) Correlation of O–H stretching frequencies and O-H···O hydrogen bond lengths in minerals. *Monatshefte für Chemie*, **130**, 1047–1059.

Mandarino, J.A. (1976) The Gladstone-Dale relationship – Part 1: derivation of new constants. *Canadian Mineralogist*, **14**, 498–502.

Mandarino, J.A. (2007) The Gladstone–Dale compatibility of minerals and its use in selecting mineral species for further study. *Canadian Mineralogist*, **45**, 1307–1324.

Pekov, I.V., Krivovichev, S.V., Yapaskurt, V.O., Chukanov, N.V., and Belakovskiy, D.I. (2014) Beshtauite, $(NH_4)_2(UO_2)(SO_4)_2 \cdot 2H_2O$, a new mineral from Mount Beshtau, Northern Caucasus, Russia. *American Mineralogist*, **99**, 1783–1787.

Plášil, J. (2014) Oxidation–hydration weathering of uraninite: the current state-of-knowledge. *Journal of Geoscience*, **59**, 99–114.

Plášil, J., Hloušek, J., Kasatkin, A.V., Novák, M., Čejka, J. and Lapčák, L. (2015) Svornostite, $K_2Mg[(UO_2)(SO_4)_2]_2 \cdot 8H_2O$, a new uranyl sulfate mineral from Jáchymov, Czech Republic. *Journal of Geosciences*, **60**, 113–121.

Plášil, J., Kampf, A.R., Ma, C., Desor, J. (2023) Oldsite, $K_2Fe^{2+}[(UO_2)(SO_4)_2]_2(H_2O)_8$, a new uranyl sulfate mineral from Utah, USA: its description and implications for the formation and occurrences of uranyl sulfate minerals. *Mineralogical Magazine*, **87**, 151–159.

Sheldrick, G.M. (2015a) SHELXT - Integrated space-group and crystal-structure determination. *Acta Crystallographica*, **A71**, 3–8.

Sheldrick, G.M. (2015b) Crystal Structure refinement with *SHELX*. *Acta Crystallographica*, **C71**, 3–8.

Tabachenko, V.V., Serezhkin, V.I., Serezhkina, L.B. and Kovba, L.M. (1979) Crystal structure of manganese sulfatouranylate $MnUO_2(SO_4)_2(H_2O)_5$. *Soviet Journal of Coordination Chemistry*, **5**, 1219–1223.

FIGURE CAPTIONS

Figure 1. Yellow blades of svornostite-(NH_4) with hexahydrite (white) and plášilite (greenish yellow blades in upper right) on kröhnkite; cotype specimen #76445. The field of view is 1.14 mm across.

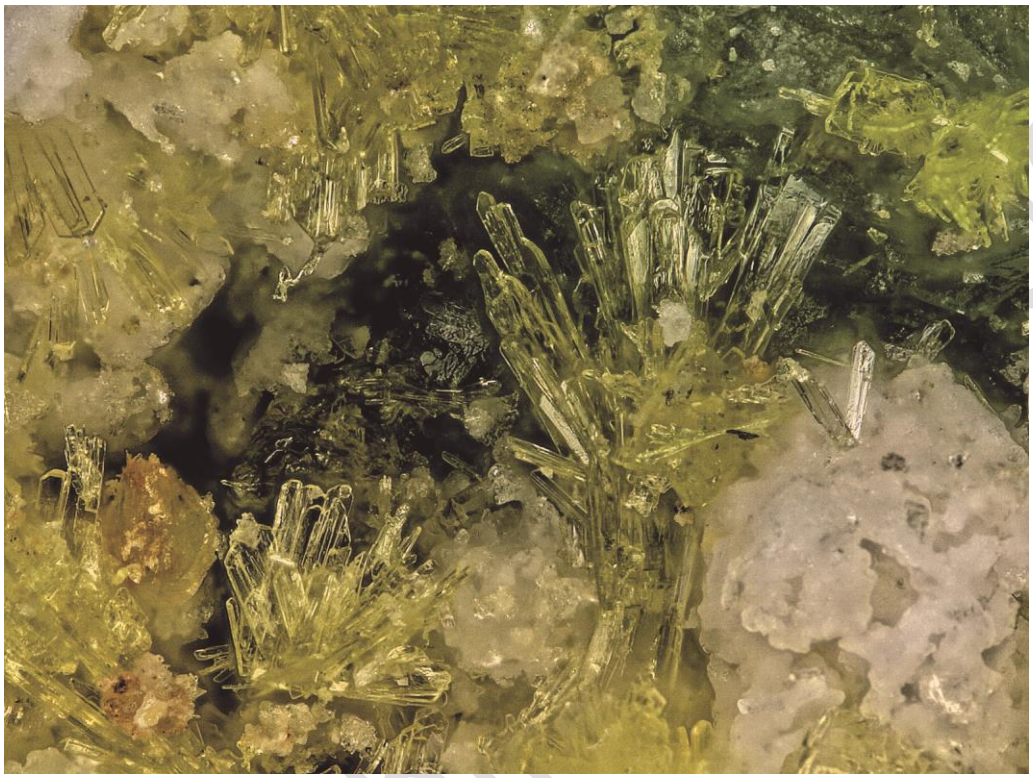

Figure 2. Crystal drawing of svornostite-(NH_4); clinographic projection. The drawing was created using SHAPE, version 7.4 (Shape Software, Kingsport, Tennessee, USA).

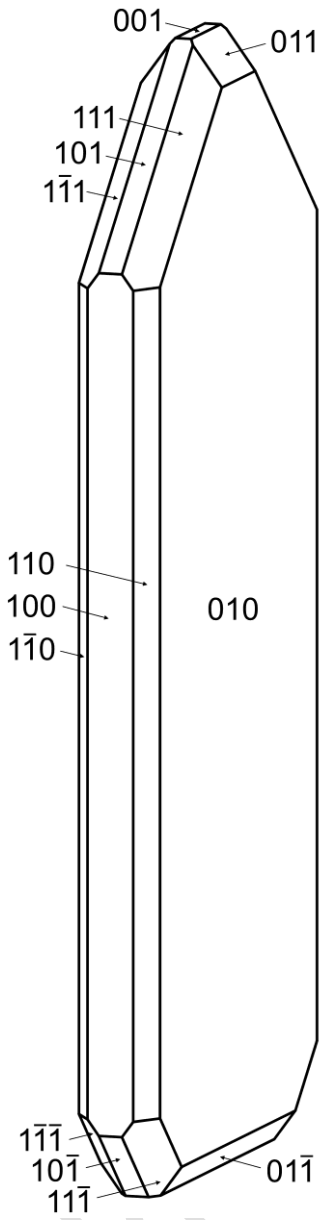

Figure 3. Raman spectrum of svornostite-(NH_4).

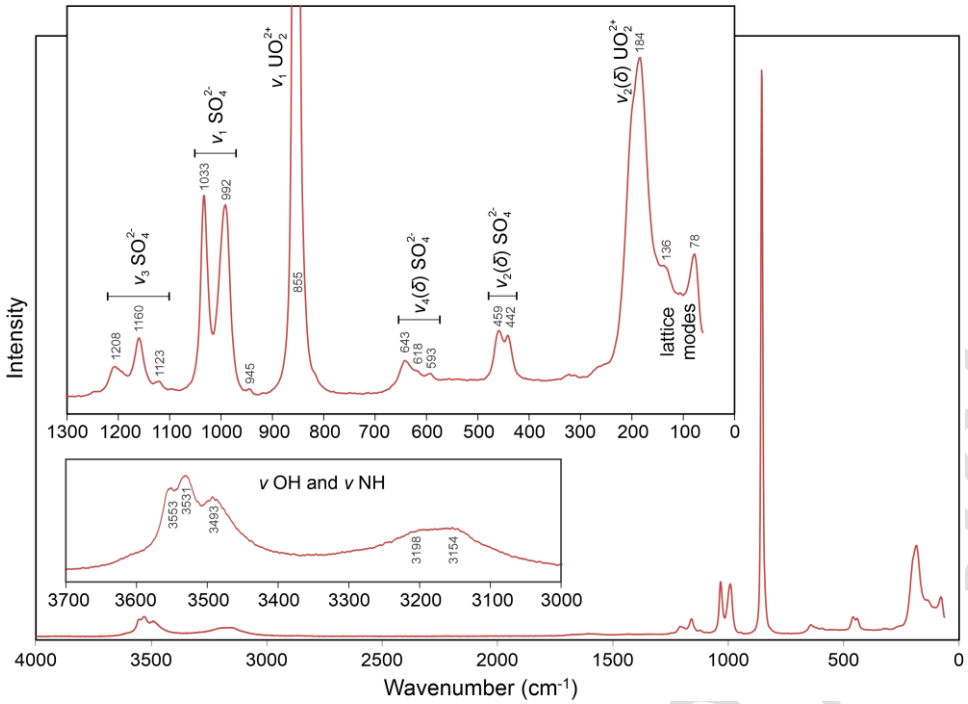

Figure 4. FTIR spectrum of svornostite-(NH_4).

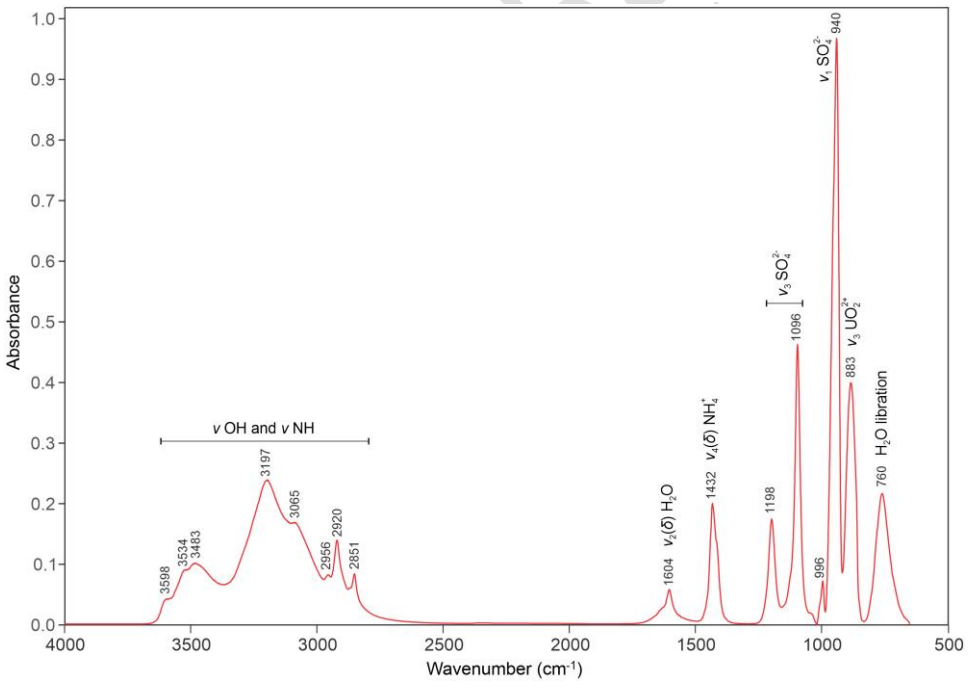

Figure 5. Portion of LIBS spectrum showing N I lines. The red curve is for svornostite-(NH_4); the blue curve is the background.

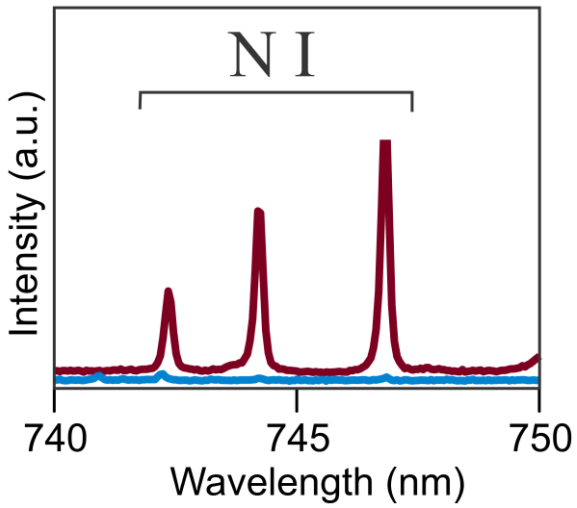

Figure 6. The uranyl sulfate chains in the structures of svornostite-(NH_4), oppenheimerite and bobcookite.

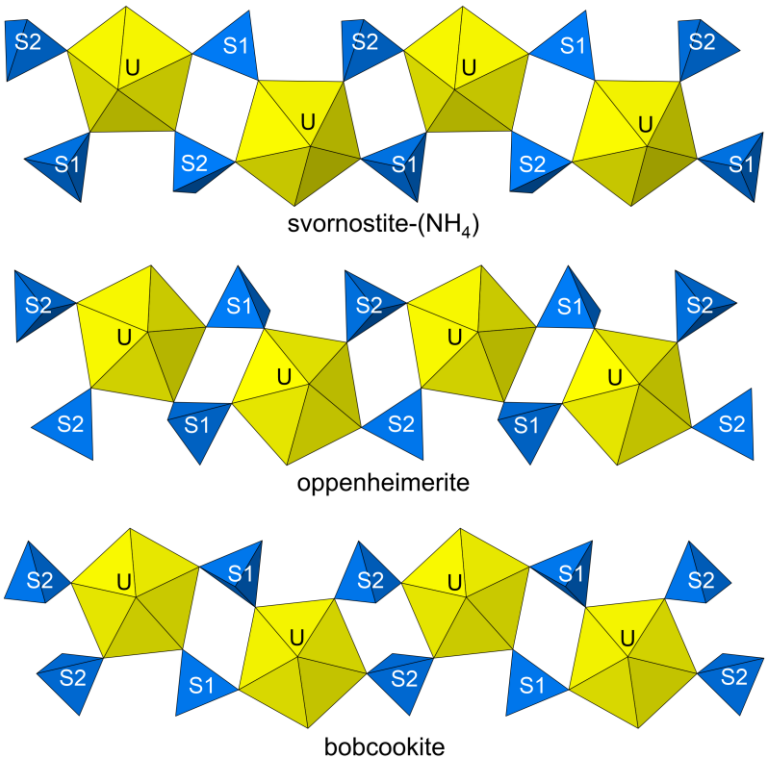

Figure 7. The structures of svornostite-(NH_4) and rietveldite viewed down [010]. The unit-cell outline is shown by dashed lines. The figures were created using ATOMS, version 6.5 (Shape Software, Kingsport, Tennessee, USA).

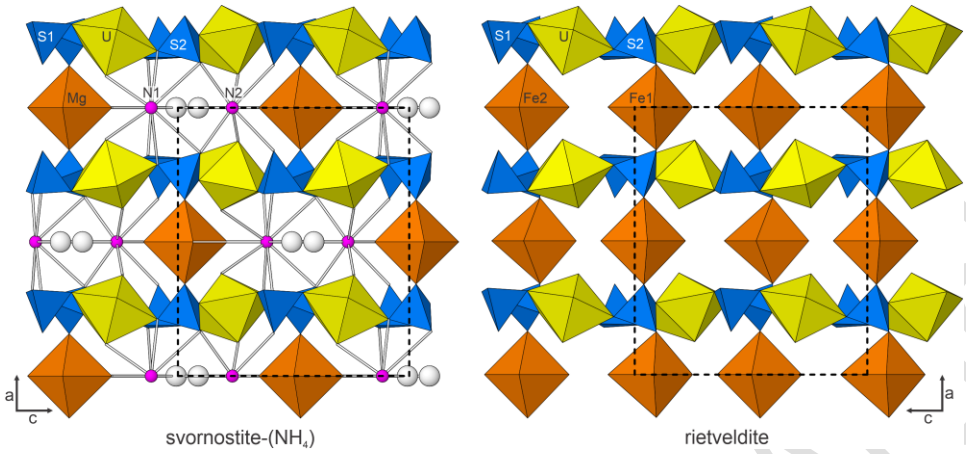

Figure 8. The x = 0 layers in the structures of svornostite-(NH_4) and rietveldite. Note that the N1 and N2 sites are depicted as large balls to represent the large size of the NH_4 groups, which are in approximately the same locations as the K cations in the svornostite-(K) and oldsite-(K) structures. The unit-cell outlines are shown by dashed lines.

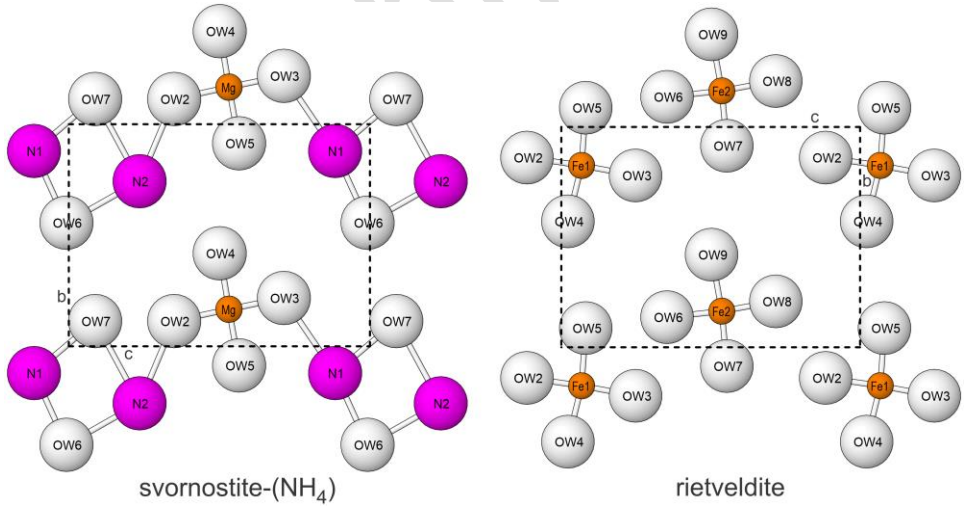

Table 1. Comparison of selected data for minerals in the svornostite group.

	Svornostite subgroup			Rietveldite subgroup	
	Svornostite-(NH_4)	Svornostite-(K)	Oldsite-(K)	Rietveldite	Zincorietveldite
Ideal formula*	$(NH_4)_2Mg(UO_2)_2(SO_4)_4(H_2O)_8$	$K_2Mg(UO_2)_2(SO_4)_4(H_2O)_8$	$K_2Fe(UO_2)_2(SO_4)_4(H_2O)_8$	$Fe_2(UO_2)_2(SO_4)_4(H_2O)_{10}$	$Zn_2(UO_2)_2(SO_4)_4(H_2O)_{10}$
Crystal system	orthorhombic	orthorhombic	orthorhombic	orthorhombic	orthorhombic
Space group	$Pmn2_1$	$Pmn2_1$	$Pmn2_1$	$Pmn2_1$	$Pmn2_1$
a (Å)	13.0259(9)	12.7850(3)	12.893(3)	12.9577(9)	12.8712(9)
b (Å)	8.2909(4)	8.2683(4)	8.276(2)	8.3183(4)	8.3148(4)
c (Å)	11.2589(4)	11.2163(3)	11.239(2)	11.2971(5)	11.3148(4)
V (Å^3)	1215.92(11)	1185.68(7)	1199.2(5)	1217.67(11)	1208.90(11)
Z	2	2	2	2	2
Reference	*This work*	Plášil *et al.*, 2015	Plášil *et al.*, 2023	Kampf *et al*., 2017	Kampf *et al*., 2023

* Note that the formulas of rietveldite and zincorietveldite are given for $Z = 2$ instead of $Z = 4$ for the sake of comparison with the other svornostite-group minerals.

Table 2. Analytical data (in wt.%) for svornostite-(NH_4).

Constituent	Mean	Range	S.D.	Standard
$(NH_4)_2O$*	4.17			
Na_2O	0.17	0.14–0.20	0.03	albite
K_2O	0.16	0.14–0.17	0.01	microcline
MgO	2.57	2.39-2.76	0.19	forsterite
MnO	1.51	1.22-1.66	0.20	Mn_2SiO_4
SO_3	27.11	26.86-27.22	0.17	anhydrite
UO_3	48.17	47.57-48.87	0.56	UO_2
H_2O*	12.17			
Total	96.03			
* Based on structure				

Table 3. Data collection and structure refinement details for svornostite-(NH_4).

Diffractometer	Rigaku R-Axis Rapid II
X-ray radiation/power	Mo$K\alpha$ (λ = 0.71075 Å)/50 kV, 40 mA
Temperature	293(2) K
Formula from SREF	$(NH_4)_2(Mg_{0.749}Mn_{0.251})(UO_2)_2(SO_4)_4(H_2O)_8$ (incl. unlocated H)
Space group	$Pmn2_1$ (#31)
Unit cell dimensions	a = 13.0259(9) Å
	b = 8.2909(4) Å
	c = 11.2589(4) Å
V	1215.92(11) Å^3
Z	2
Density (for above formula)	3.082 g cm^{-3}
Absorption coefficient	13.910 mm^{-1}
F(000)	1034.5
Crystal size	100 × 60 × 15 μm
θ range	3.05 to 27.44°
Index ranges	$-16 \le h \le 16$, $-10 \le k \le 10$, $-14 \le l \le 12$
Reflections collected/unique	11165/2590; R_{int} = 0.035
Reflections with $I > 2\sigma_I$	2222
Completeness to θ = 27.44°	99.7%
Refinement method	Full-matrix least-squares on F^2
Parameter/restraints	182/1
GoF	1.100
Final R indices [$I > 2\sigma_I$]	R_1 = 0.0243, wR_2 = 0.0524
R indices (all data)	R_1 = 0.0315, wR_2 = 0.0550
Absolute structure parameter	0.010(8)
Largest diff. peak/hole	+2.03/–1.03 e Å^{-3}

$R_{int} = \Sigma|F_o^2 - F_o^2(\text{mean})|/\Sigma[F_o^2]$. GoF = $S = \{\Sigma[w(F_o^2 - F_c^2)^2]/(n-p)\}^{1/2}$. $R_1 = \Sigma||F_o| - |F_c||/\Sigma|F_o|$. $wR_2 = \{\Sigma[w(F_o^2 - F_c^2)^2]/\Sigma[w(F_o^2)^2]\}^{1/2}$; $w = 1/[\sigma^2(F_o^2) + (aP)^2 + bP]$ where a is 0.019, b is 2.134 and P is $[2F_c^2 + \text{Max}(F_o^2, 0)]/3$.

Table 4. Atom coordinates and displacement parameters ($Å^2$) for svornostite-(NH_4).

	x/*a*	*y*/*b*	*z*/*c*	U_{eq}	U^{11}	U^{22}	U^{33}	U^{23}	U^{13}	U^{12}
N1	1/2	0.120(2)	0.384(2)	0.041(5)	0.044(11)	0.041(12)	0.038(11)	0.005(7)	0	0
N2	1/2	0.2567(15)	0.7351(15)	0.029(3)	0.013(4)	0.056(8)	0.020(8)	-0.007(8)	0	0
Mg*	0	0.1669(5)	0.5319(4)	0.0259(13)	0.0201(19)	0.031(3)	0.027(2)	-0.0001(17)	0	0
U	0.74653(2)	0.38759(3)	0.22335(17)	0.01310(9)	0.01623(14)	0.01318(15)	0.00987(14)	0.0000(3)	0.0000(2)	-0.00059(11)
S1	0.7276(2)	0.7411(4)	0.4156(2)	0.0161(6)	0.0207(10)	0.0171(15)	0.0105(13)	0.0002(11)	-0.0001(12)	0.0008(11)
S2	0.74789(16)	0.2431(4)	0.5340(2)	0.0162(7)	0.0228(13)	0.0146(15)	0.0112(14)	-0.0011(11)	0.0002(9)	0.0030(10)
O1	0.8390(4)	0.7473(10)	0.4144(7)	0.0295(16)	0.015(3)	0.040(5)	0.033(4)	-0.007(4)	0.003(3)	-0.006(3)
O2	0.6791(6)	0.8878(9)	0.3705(8)	0.031(2)	0.043(5)	0.020(5)	0.031(4)	0.014(3)	0.003(4)	0.008(3)
O3	0.6884(6)	0.6043(8)	0.3435(7)	0.0253(18)	0.037(4)	0.018(4)	0.021(4)	-0.010(3)	-0.003(4)	0.004(3)
O4	0.6885(5)	0.7118(9)	0.5397(6)	0.0249(16)	0.031(4)	0.034(5)	0.010(3)	0.005(3)	0.002(3)	0.002(3)
O5	0.8429(5)	0.1500(9)	0.5296(7)	0.0277(18)	0.019(3)	0.026(5)	0.038(5)	-0.003(4)	-0.002(3)	0.005(3)
O6	0.7707(8)	0.4005(11)	0.5903(10)	0.048(3)	0.080(8)	0.031(5)	0.033(5)	-0.013(4)	-0.011(5)	0.010(4)
O7	0.6678(5)	0.1564(10)	0.5961(7)	0.034(2)	0.026(4)	0.041(5)	0.035(4)	0.020(4)	0.016(4)	0.007(3)
O8	0.7112(5)	0.2751(9)	0.4116(6)	0.0247(15)	0.036(3)	0.027(4)	0.012(3)	0.003(3)	-0.007(3)	0.000(3)
O9	0.6184(5)	0.3385(9)	0.1884(5)	0.0245(16)	0.024(3)	0.030(4)	0.020(4)	-0.007(3)	0.000(3)	-0.001(3)
O10	0.8760(4)	0.4333(9)	0.2603(6)	0.0258(16)	0.023(3)	0.027(4)	0.027(4)	-0.011(3)	0.000(3)	-0.001(3)
OW1	0.7915(6)	0.0962(7)	0.2362(9)	0.0297(17)	0.052(4)	0.012(3)	0.025(5)	-0.003(3)	0.010(5)	-0.001(3)
OW2	0	0.1136(19)	0.3498(17)	0.046(5)	0.048(10)	0.050(12)	0.041(11)	-0.002(7)	0	0
OW3	0	0.2176(15)	0.7141(16)	0.047(3)	0.030(5)	0.086(9)	0.026(6)	-0.006(9)	0	0
OW4	0	0.4189(13)	0.5012(11)	0.037(3)	0.040(6)	0.028(7)	0.044(7)	-0.004(5)	0	0
OW5	0	0.9140(18)	0.5656(18)	0.037(4)	0.021(6)	0.021(7)	0.068(11)	0.007(6)	0	0
OW6	1/2	0.4433(16)	0.4922(12)	0.051(3)	0.039(6)	0.050(9)	0.063(9)	0.003(7)	0	0
OW7	1/2	0.886(2)	0.5875(18)	0.050(5)	0.029(8)	0.079(14)	0.040(10)	0.000(8)	0	0

* Refined occupancy: $Mg_{0.749(16)}Mn_{0.251(16)}$

Table 5. Selected bond distances (Å) for svornostite-(NH_4).

N1–OW6	2.94(2)	U–O9	1.762(6)	Mg–O5	2.052(7)
N1–OW7	3.00(2)	U–O10	1.778(6)	Mg–O5	2.052(7)
N1–O2	3.032(14)	U–O6	2.320(9)	Mg–OW3	2.094(18)
N1–O2	3.032(14)	U–O8	2.361(7)	Mg–OW2	2.10(2)
N1–O8	3.050(10)	U–O3	2.373(7)	Mg–OW4	2.117(12)
N1–O8	3.050(10)	U–O4	2.381(7)	Mg–OW5	2.131(15)
N1–O9	3.243(19)	U–OW1	2.490(6)	<Mg–O>	2.091
N1–O9	3.243(19)	<U–O_{Ur}>	1.770		
N1–O7	3.248(19)	<U–O_{eq}>	2.385	*Hydrogen bonds*	
N1–O7	3.248(19)			OW1···O2	2.723(11)
N1–OW3	3.40(2)	S1–O1	1.453(6)	OW1···O7	2.675(11)
<N1–O>	3.135	S1–O2	1.461(8)	OW2···O10 (×2)	3.264(15)
		S1–O3	1.485(8)	OW3···O2 (×2)	3.051(14)
N2–O7	2.814(12)	S1–O4	1.507(7)	OW4···O5 (×2)	3.043(11)
N2–O7	2.814(12)	<S1–O>	1.468	OW5···O1 (×2)	3.034(15)
N2–O1	2.911(14)			OW6···O3 (×2)	3.257(11)
N2–O1	2.911(14)	S2–O7	1.447(8)	OW7···O4 (×2)	2.900(12)
N2–O10	3.049(13)	S2–O5	1.459(7)		
N2–O10	3.049(13)	S2–O6	1.481(10)		
N2–OW6	3.14(2)	S2–O8	1.484(8)		
N2–OW2	3.33(2)	<S1–O>	1.477		
N2–OW7	3.49(2)				
<N2–O>	3.056				

Table 6. Bond valence analysis for svornostite-(NH_4). Values are expressed in valence units.*

	N1(NH_4)	N2(NH_4)	Mg	U	S1	S2	Hydrogen bonds		Σ_{anion}
							Accepted	Donated	
O1		$0.16^{\times 2\downarrow}$			1.57		0.12		1.85
O2	$0.11^{\times 2\downarrow}$				1.54		0.22, 0.12		1.99
O3				0.50	1.45		0.10		2.05
O4				0.49	1.37		0.15		2.01
O5			$0.39^{\times 2\downarrow}$			1.55	0.12		2.06
O6				0.56		1.47			2.03
O7	$0.06^{\times 2\downarrow}$	$0.20^{\times 2\downarrow}$				1.60	0.24		2.10
O8	$0.11^{\times 2\downarrow}$			0.51		1.46			2.08
O9	$0.06^{\times 2\downarrow}$			1.82					1.88
O10		$0.11^{\times 2\downarrow}$		1.76			0.10		1.97
OW1				0.39				-0.22, -0.24	-0.07
OW2		0.05	0.35					$-0.10^{\times 2\rightarrow}$	0.20
OW3	0.04		0.36					$-0.12^{\times 2\rightarrow}$	0.16
OW4			0.34					$-0.12^{\times 2\rightarrow}$	0.10
OW5			0.33					$-0.12^{\times 2\rightarrow}$	0.09
OW6	0.15	0.08						$-0.10^{\times 2\rightarrow}$	0.03
OW7	0.12	0.03						$-0.15^{\times 2\rightarrow}$	-0.15
Σ_{cation}	0.99	1.10	2.16	6.03	5.93	6.08			

* Multiplicity is indicated by $\times\rightarrow\downarrow$. NH_4^+–O bond-valence parameters from Garcia-Rodriguez *et al*. (2000). Mg^{2+}–O, U^{6+}–O and S^{6+}–O bond-valence parameters are from Gagné and Hawthorne (2015). Hydrogen-bond strengths based on O–O bond lengths from Ferraris and Ivaldi (1988).